Study on Anti-explosion Performance of Steel Beam-slab Protective Doors

Ziye Liu[a], Xianxiang Zhou[b], Fantong Lin[c], Xiao Li[d], Lan Xiao[e*]

National Defense Engineering Research Institute, Academy of Military Sciences, Beijing, China

[a]lzyy0011@163.com,[b]zhouxianxiang1@163.com,
[c]linfantong@126.com,[d]2494921428@qq.com,[e*]festoon@sina.com

Abstract. To investigate the anti-explosion performance of steel beam-slab protective door under underwater explosion impact, a three-dimensional numerical model for the steel beam-slab protective door under underwater impact load was established, and the effects of constraint conditions, height and thickness of the flat web in the skeleton beam, width and thickness of the flange plate on its anti-explosion performance were analyzed. The calculation results demonstrate that the frame beam at the edge of the protective door is the most vulnerable component in terms of anti-explosion performance. It is susceptible to various failure modes, including buckling deformation of local frame beam, overall flexural failure, compression-bending failure, and warping failure of frame beams on both sides; the variation in constraint conditions has a notable influence on the anti-explosion performance of the structure; increasing the height and thickness of the flat web results in a reduction of approximately 20% in the peak displacement of the structure. But simply increasing the width and thickness of the flange plate has a limited impact on the structural resistance to explosions.

Keywords: underwater explosion; protective door; anti-explosion performance; failure mode.

1 Introduction

Underwater explosions release a significant amount of energy within a confined range, causing a strong shock wave that poses a serious threat to the safety of hydraulic structures. [1-3]. Hydraulic structures serve crucial functions in various sectors, including power generation, flood control, water supply, and navigation, representing important national resources, which are vulnerable to explosions and other attacks. In the midst of an explosion, the hydraulic structure is susceptible to the shock wave, with its mouth often being the primary target, and once it is destroyed, it will cause damage to the inside of the structure. As the most important protective equipment at the mouth, the protective door plays a decisive role in the safety of underwater engineering. Therefore, it is of great significance to study the anti-explosion performance of underwater protective doors.

P. Xiang et al. (eds.), *Proceedings of the 2023 5th International Conference on Hydraulic, Civil and Construction Engineering (HCCE 2023)*, Atlantis Highlights in Engineering 26,
https://doi.org/10.2991/978-94-6463-398-6_73

The structural form of the steel protective door mainly consists of a beam-slab configuration, that is, the skeleton beam is taken as the main stress component, supplemented by panel support [4]. Steel plate or I-beam can be used for skeleton beams. When the explosion load acts on the protective door, the skeleton beam can absorb most of the explosion energy and effectively improve the anti-explosion performance of the protective door. Admittedly, the majority of current studies only focus on the analysis of the anti-explosion performance of beam-slab protective doors under explosion load in the air [5-7]. However, the beam-slab structure shares similarities with the stiffened plate structure. By studying the anti-explosion performance of the stiffened plate, the dynamic response characteristics of the underwater explosion to the beam-slab protective door can be obtained. Jen et al. studied the transient response of stiffened plate structures with different sizes to underwater impact load and proposed damage factors that can be used to describe the damage degree of stiffened plate structures [8]. According to Hains acoustic approximation method, Jiang et al. put forward a simplified analysis method for predicting the nonlinear dynamic response of stiffened plates under underwater explosion, which can well analyze the rigid-plastic behavior of unidirectional and bidirectional stiffened plates [9]. Gupta et al. obtained the failure modes of stiffened and unstiffened plates under underwater explosion load by numerical simulation and analyzed the influence of plate thickness on the failure modes [10]. Elsayed et al. conducted a numerical analysis to obtain the dynamic response of a stiffened plate subjected to underwater explosion loads. The results of their analysis revealed that considering the strain rate effect of materials can effectively reduce the displacement of stiffened plates [11]. The above research results can lay a theoretical foundation for the dynamic response analysis of beam-slab protective doors under underwater explosion.

This paper aims to delve deeper into the dynamic response characteristics of a steel beam-slab protective door when subjected to underwater explosion loads. Numerical simulations allow for analyzing the dynamic response and resistance of the steel beam-slab protective door under such loads. The study takes into account the influences of constraint conditions, height and thickness of the flat web in the skeleton beam, as well as the width and thickness of the flange plate on the anti-explosion performance of the structure.

2 Analysis of Resistance Performance of Steel Beam-slab Protective Doors

2.1 Finite element modeling

The door leaf of the beam-slab protective door has a size of 4 × 5.5 × 0. 686 m (length × width × height). The inner skeleton beam of the door leaf is composed of I-beams, arranged in a grid pattern with 7 beams in the longitudinal direction and 10 beams in the transverse direction, and the periphery is connected by steel plates. The thickness of the upper and lower panels and the surrounding support panels of the skeleton beam is 28 mm, and the skeleton beam is made of 63C I-beams, as outlined in Figure 1. Compared with traditional steel, high-strength steel displays notable advantages such

as high yield strength and better energy absorption capacity [12], so Q690 high-strength steel is selected as the protective door material. Its parameters include an elastic modulus of 2.06 × 1011 Pa, a density of 7850 kg/m^3, and ultimate strength of 770 MPa.

The finite element model of the steel beam-slab protective door, as depicted in Figure 2, utilizes a Lagrange mesh for accurate representation, with a division of 193,416 elements. In the calculation, the general contact algorithm is adopted to consider the contact between the explosion-facing and back-explosion surface and the skeleton beam and surrounding support panels, respectively. It is important to note that the current study focuses solely on the dynamic response of the door body, and thus the influence of surrounding components, such as the door frame, has been neglected. Additionally, for simplification purposes, the four sides of the door body are assumed to be simply supported.

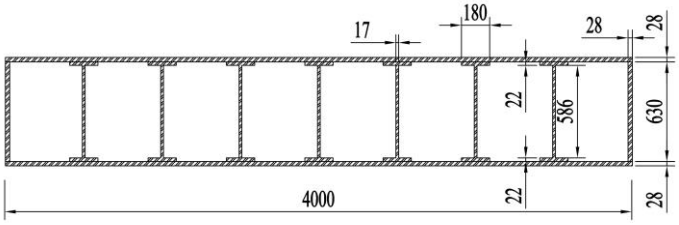

(a) Cross-sectional view of the protective door along the width

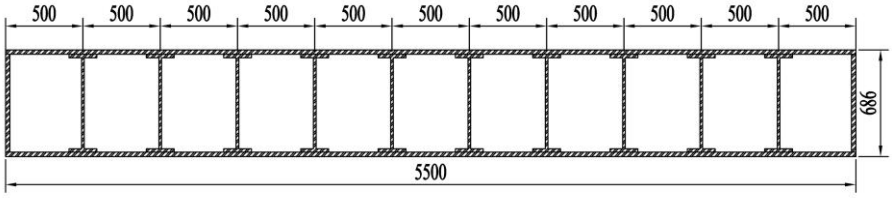

(b) Cross-sectional view of the protective door along the length

Fig. 1. Cross-sectional views of steel beam-slab protective door (dimension unit: mm)

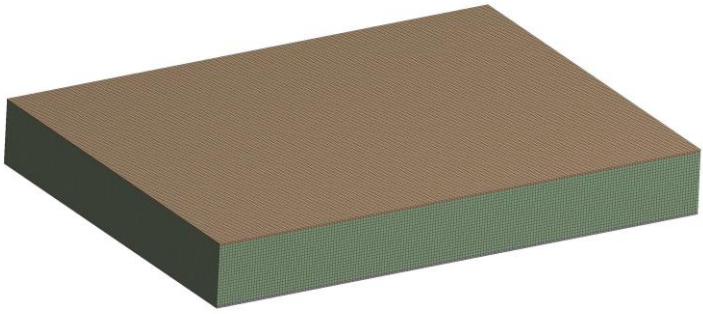

(a) Finite element model drawing of the outer panel of the protective door

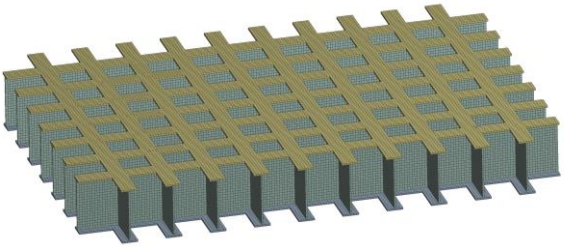

(b) Finite element model drawing of skeleton beam

Fig. 2. Finite element model of steel beam-slab protective door

2.2 Material models

High-strength steel Q690 will undergo hardening under a high strain rate. The John-Cook model adopted different strengthening criteria and considered the effects of strain hardening, strain rate hardening, and temperature softening, the research under which can simulate the response of most metal materials under explosion load [13]. Likewise, this paper introduces the dynamic characteristics of high-strength steel materials, defining the yield stress as:

$$\sigma=\left[A+B\left(\varepsilon^{p}\right)^{n}\right]\left(1+C\bullet\ln\frac{\varepsilon_{p}'}{\varepsilon_{1}'}\right)\left(1+T^{*m}\right) \tag{1}$$

In this equation, A is the yield stress; B is the strain hardening constant; C is a strain rate sensitive parameter; n is the strain hardening exponent; ε^{p} and ε_{p}' are plastic strain and plastic strain rate; ε_{1}' is the reference strain rate; $T^{*m}=\left(T-Tr\right)\left(Tm-Tr\right)$, where m is the temperature softening index. Specific parameters are referred to the study conducted by Yang et al. [14], as shown in Table 1.

Table 1. John-Cook model parameters of high-strength steel

A/MPa	B/MPa	n	C	m
722	400	0.57	0.021	-

When the material is under pressure, by employing the Gruneisen equation of state, it is possible to describe the water medium, where the explosive impact load propagates:

$$p_{H}=\frac{\rho_{0}C_{0}^{2}\mu\left[1+\left(1-\frac{\gamma_{0}}{2}\mu-\frac{a\mu^{2}}{2}\right)\right]}{\left[1-\mu\left(S_{1}-1\right)-\frac{\mu^{2}S_{2}}{\mu+1}-\frac{\mu^{2}S_{3}}{\left(\mu+1\right)^{2}}\right]^{2}}+\left(\gamma_{0}+a\mu\right)E_{V} \tag{2}$$

The equation of state in the event of material expansion is:

$$p = \rho_0 C_0^2 \mu + (\gamma_0 + a\mu) E_V \tag{3}$$

where E_V is the initial internal energy per unit volume; a is a constant, which is the first-order volume correction coefficient of γ_0. Table 2 details the parameters of the Grunesien equation of state used in the simulation.

Table 2. Parameters of Grunesien equation of state

C/cm· μ s^{-1}	S_1	S_2	S_3	a	γ_0	ρ /g·cm^{-3}
0.1647	1.921	-0.096	0	0	0.35	1.0

Jones-Wilkins-Lee (JWL) equation of state is used to describe the pressure generated by chemical energy in the explosion, which defines the pressure as a function of relative specific volume V and specific internal energy e of detonation products:

$$p = A\left(1 - \frac{\omega}{VR_1}\right)e^{-VR_1} + B\left(1 - \frac{\omega}{VR_2}\right)e^{-VR_2} + \frac{\omega e}{V} \tag{4}$$

where p is the detonation product; V is the relative specific volume of detonation products, and $V = v / v_0$; A, B, R_1, R_2 and ω are the parameters to be fitted, and the related parameters in the JWL equation of state are described in Table 3.

Table 3. Parameters of JWL equation of state

ρ /km·m^{-1}	D /m·s^{-1}	P_{CJ}/GPa	A/GPa	B/GPa	R_1	R_2	ω
1630	6717	18.5	373.8	3.75	4.15	0.9	0.35

2.3 Determination of explosion load

The protective door is in an underwater environment, where the explosion-facing surface of the protective door faces the water and the back-explosion surface faces the air. We selected the explosive equivalents as 200 kg, 300 kg, 400 kg, and 500 kg, the initiation distance as 10 m, and the action time as 30 ms.

2.4 Dynamic response analysis of protective doors

To explore the damage process of steel beam-slab protective door under underwater explosion impact load, the impact load was applied to the protective door when the explosive equivalent was 500 kg and the explosion distance was 10 m. Figure 3 shows the equivalent stress of the protective door at different times. When t=4.8 ms, the explosion impact load began to act on the explosion-facing panel. Then the stress on the

panel was transferred to the skeleton beam. When t=5.5 ms, the stress concentrated at the flat web of the skeleton beam around, which made the skeleton beam under pressure. At this time, the maximum equivalent stress value was about 820.1 MPa, which exceeded the ultimate strength of the material, as shown in Figure 3 (b); as time progresses, when t=7 ms, the compressive damage at the flat web of the skeleton beam developed further, and the stress gradually developed from the periphery of the skeleton beam to the central area, as plotted in Figure 3 (c). At this time, the maximum equivalent stress was about 920.6 MPa, and some skeleton beams have been subjected to buckling deformation; because the attenuation speed of explosion pressure in water is slower than that in air, and the explosion impact load continues to act on the protective door, the protective door bears a larger distributed load, which leads to the bending deformation of the whole protective door. When t=13 ms, the protective door has obvious buckling deformation. As illustrated in Figure 3 (d), the stress value at the junction of the flat web in the skeleton beam and upper flange plate was the highest, reaching a maximum value of approximately 1039 MPa. At this point, the protective door was already in a plastic deformation state. As the reflected shock wave propagated in water, the reflected sparse wave gradually formed, and the structure moved in the opposite direction of the shock wave propagation. Under the superposition action of different wave systems, the structure of the protective door was constantly deformed. When t=30 ms, the protective door collapsed to the central area, and the skeleton beams around it have been buckled and destroyed. From Figure 3 (e), it is evident that the resistance of the protective door has become significantly insufficient, leading to plastic failure.

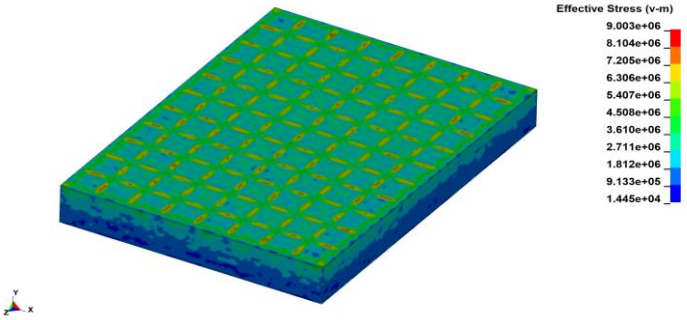

(a) 4.8 ms

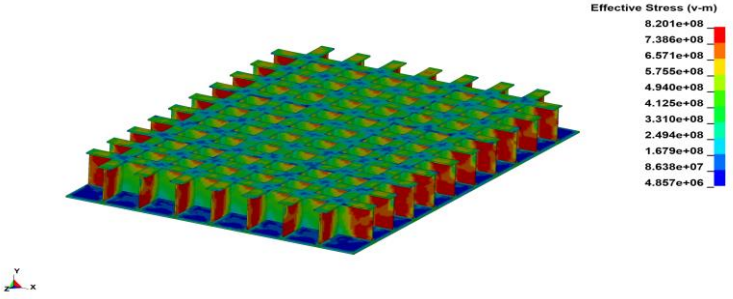

(b) 5.5 ms

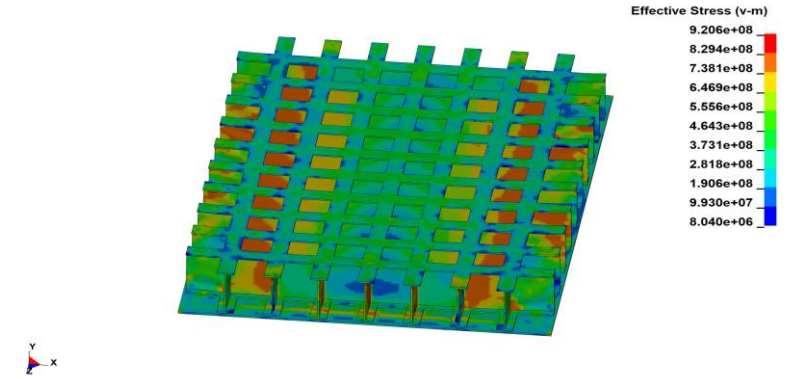

(c) 7 ms

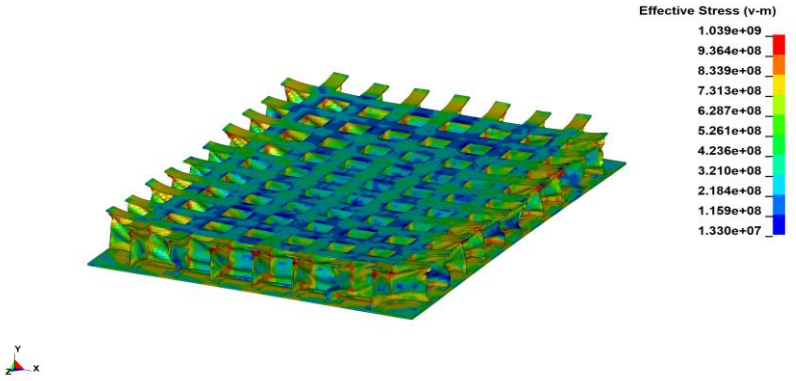

(d) 13 ms

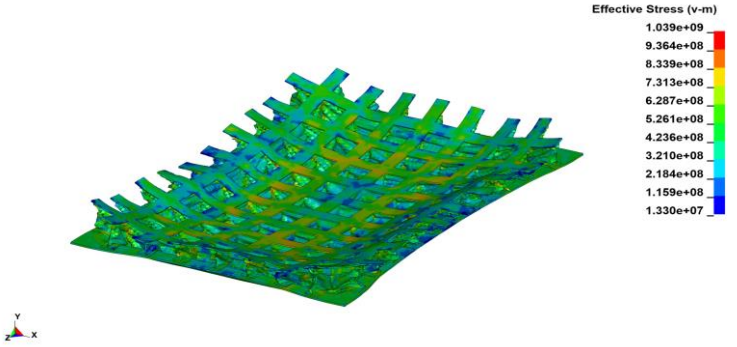

(e) 30 ms

Fig. 3. Mises stress at different times

Figure 4 depicts the equivalent plastic strain of the protective door at different times. The change process of equivalent plastic strain on the door leaf of the protective door closely resembles that of equivalent stress. When t=5.5 ms, the equivalent plastic strain

on the upper and lower sides of the flat web of the skeleton beam appeared for the first time, and its strain value was about 8.427×10^{-3}, as shown in Figure 4 (a); under the continuous impact load exerted on the structure, the protective door undergoes ongoing bending and deformation along the propagation direction of the shock wave. When t=26.2 ms, as observed in Figure 4 (b), the maximum plastic strain mainly appeared at the flat web of the surrounding skeleton beam and tended to develop towards the central area. In the meantime, the protective door reached the maximum displacement, and the maximum equivalent plastic strain was about 1.284, suggesting that the door body completely entered the plastic stage; when t=30 ms, the damage development essentially comes to a halt. It is notable from Figure 4 (c) that the flat web in the central region of the skeleton beam is the weak part of the whole structure, and the maximum equivalent plastic strain is about 1.285.

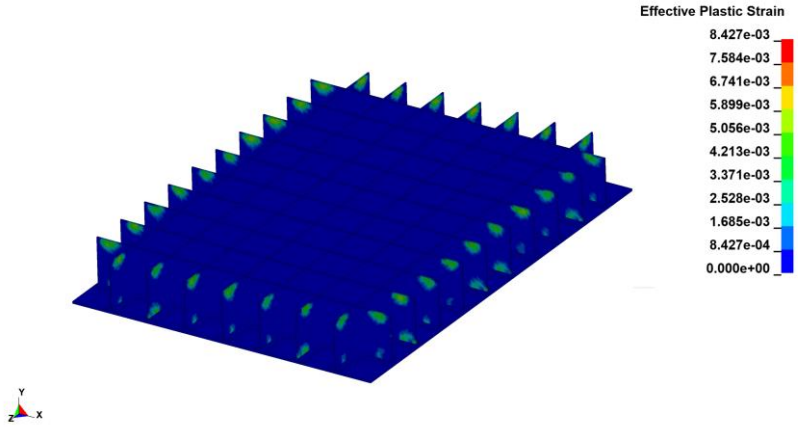

(a) 5.5 ms

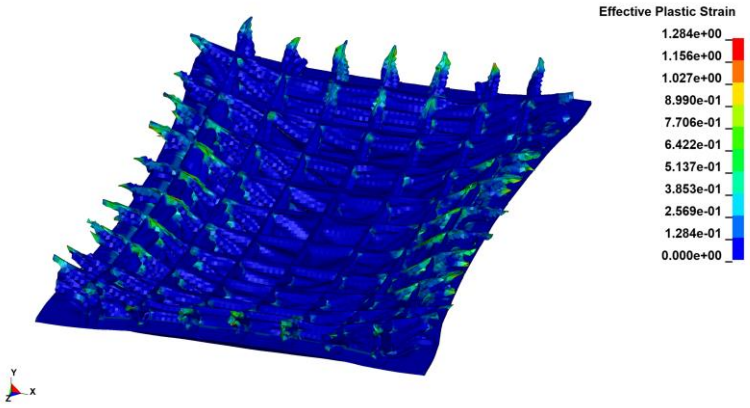

(b) 26.2 ms

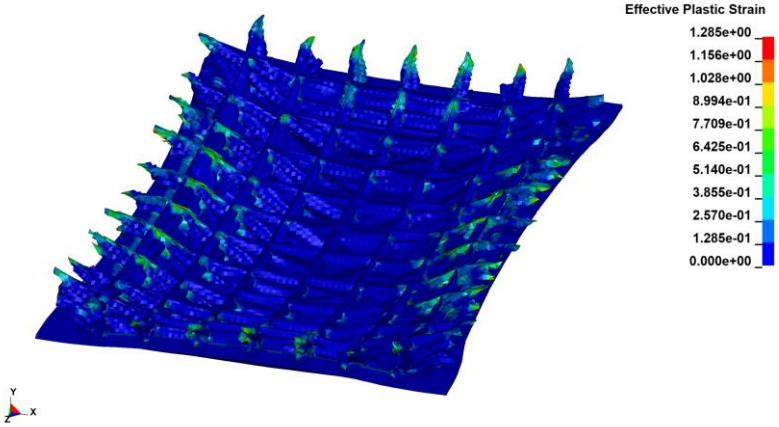

(c) 30 ms

Fig. 4. Equivalent plastic strain at different times

3 Analysis of Influencing Factors of Steel Beam-slab Protective Door

3.1 Influence of constraint conditions on door leaf resistance

To explore the influence of constraint conditions on the resistance of the protective door, the constraint conditions are set as: four-side simply supported constraint and three-side simply supported constraint respectively. Among them, the three-side simply supported restraint is posed on both sides and the bottom of the protective door. Because in the vertical closed protective door, when the protective door is closed, there are door frames on both sides and bottom to restrain it. The explosive equivalents were set as 200 kg, 300 kg, 400 kg, and 500 kg respectively, and the initiation distance as 10 m, while other structural parameters remained unchanged.

Figure 5 provides a visual representation of the failure mode and stress distribution of the protective door under different constraints. In Figures 5 (a) and (b), which correspond to explosive equivalents of 200 kg to 300 kg, the failure mode of the protective door under both constraint configurations exhibited buckling deformation of the local skeleton beam, the whole structure was in an elastic state, and the maximum equivalent stress values of the protective door were about 579.2 MPa and 765.3 MPa respectively. With the increase of explosive equivalent, the impact load of the protective door gradually increases. As observed in Figure 5 (c), in the case of a four-side simply supported constraint, the failure mode of the protective door progressed from local buckling deformation to full compression buckling deformation of the surrounding skeleton beam, and the structure displayed overall bending failure. However, in the case of a three-side simply supported constraint, as shown in Figure 5 (d), because there is no constraint at the top of the protective door, the failure mainly occurs at the top position. With the increase in load, the displacement of the top of the protective door increases

continuously, which makes the skeleton beams on both sides break away from the original constraints and produce serious warping deformation. In Figures 5 (c) and (d), the maximum equivalent stresses of the protective door were about 987.6 MPa and 1022 MPa respectively, which have exceeded the ultimate strength of Q690 steel, and the protective door has produced large deformation.

According to the above analysis, the failure modes can be divided into three categories on account of the failure characteristics of the protective door : (1) When the explosive equivalent ranges from 200 kg to 300 kg, the failure mode of the protective door features buckling deformation of local skeleton beam; (2) When the explosive equivalent exceeds 400 kg in the case of four-side simply supported constraint, the skeleton beams around the structure are subjected to compression and bending failure, while the whole structure undergoes bending failure; (3) When the explosive equivalent exceeds 400 kg in the case of three-side simply supported constraint, the skeleton beams on both sides experiences compression and bending failure, and serious warping failure occurs on both sides of the structure.

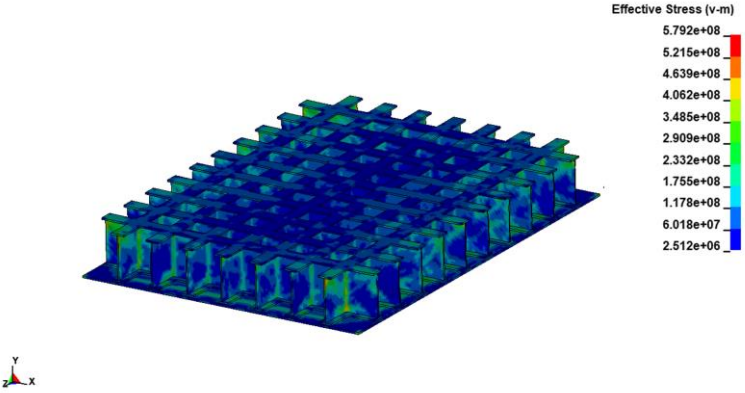

(a) Stress distribution diagram under a four-side simply supported constraint when the explosive equivalent is 200 ~ 300 kg

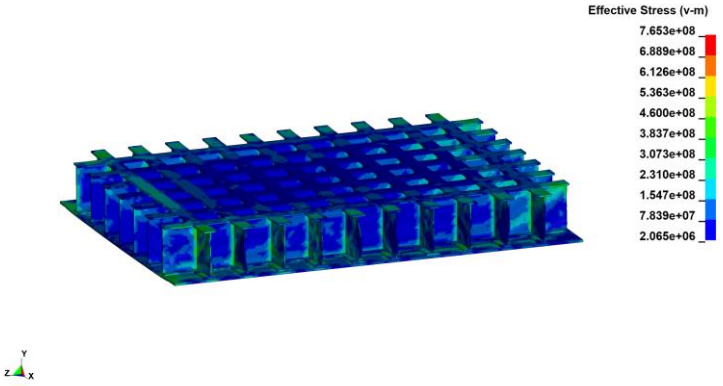

(b) Stress distribution diagram under a three-side simply supported constraint when the explosive equivalent is 200 ~ 300 kg

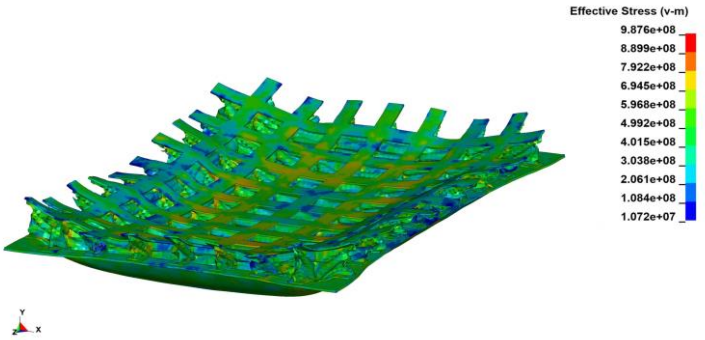

(c) Stress distribution diagram under a four-side simply supported constraint when the explosive equivalent is 400 ~ 500 kg

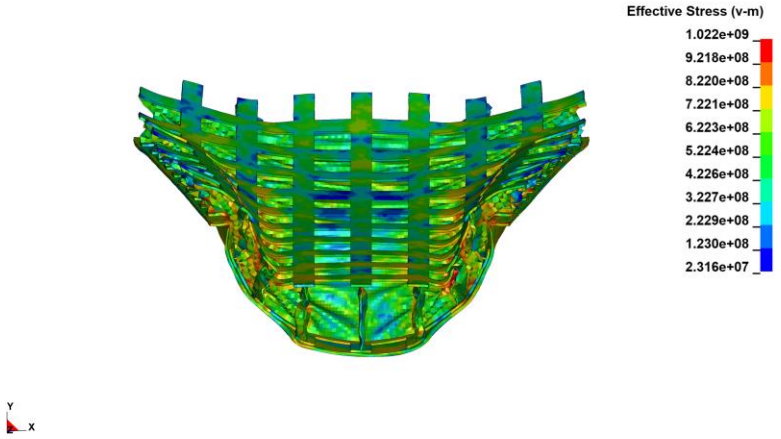

(d) Stress distribution diagram under a three-side simply supported constraint for the explosive equivalent of 400 ~ 500 kg

Fig. 5. Stress distribution diagrams of the protective door under different constraint conditions

Figure 6 (a) displays the displacement time history curve of the protective door at the center point under different explosive equivalents and two constraints. The results demonstrate that when the explosive equivalent was below 400 kg, the peak displacement of the protective door was relatively small under the two constraints. Under the condition of the four-side simply supported constraint, the peak displacements were 34.66 mm and 42.85 mm, respectively. Meanwhile, the peaks of displacement were 27.78 mm and 40.74 mm respectively under the condition of three-side simply supported constraint. After the displacement time-history curve reached the peak value, the subsequent displacement exhibited noticeable oscillations before eventually settling at a relatively fixed value. This finding indicates that after the structure reaches the peak value of displacement when it is first subjected to impact load, the stress on the structure fails to reach the limit state of the material and the structure consumes the explosion energy by its resistance, leaving it in the elastic deformation phase. However, when the

explosive equivalent was more than 400 kg, the displacement time history curves under the two constraints generally exhibited an upward trend, suggesting that after the first peak pressure of the explosion load, the structure reached the maximum bearing capacity and entered the plastic deformation stage. With the continuous application of load, the displacement growth rate and peak displacement gradually increase. Figure 6 (b) depicts the relationship between the displacement of the center point of the protective door and the explosive equivalent under two different constraint conditions. It reveals that when the explosive equivalent was less than 300 kg, the displacement difference of the center point of the protective door was small under the two constraint conditions. When the explosive equivalent reached 400 kg, the peak displacement increased rapidly. The peak displacements under the four-side constraint and three-side constraint were 648.19 mm and 1045.98 mm, respectively, with a difference of about 61.37%. When the explosive equivalent reached 500 kg, the peak displacements under the four-side constraint and three-side constraint were 771.85 mm and 1161.49 mm, respectively, with a difference of approximately 50.48%. It can be seen from the line chart that the peak displacement of the protective door under the condition of three-side constraint is much higher than that under the condition of four-side constraint, and the failure of the protective door under the condition of three-side simply supported constraint is more serious.

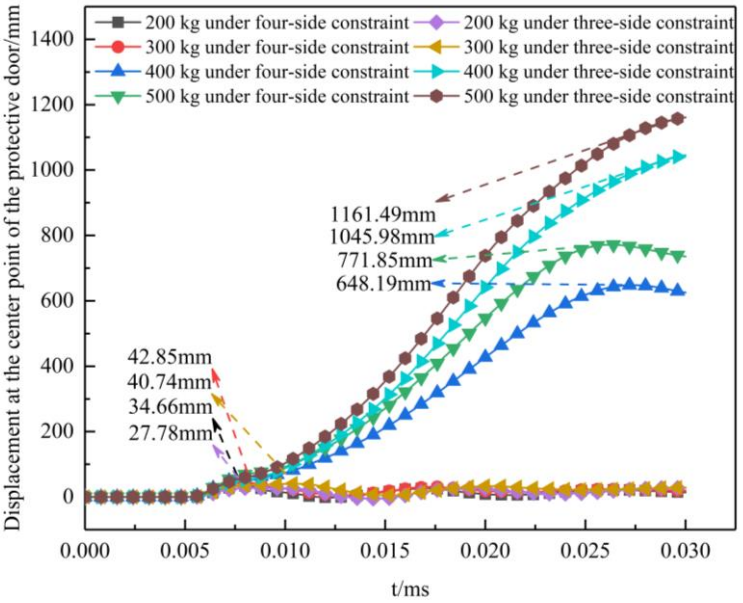

(a) Displacement time history curve of the center point of the protective door

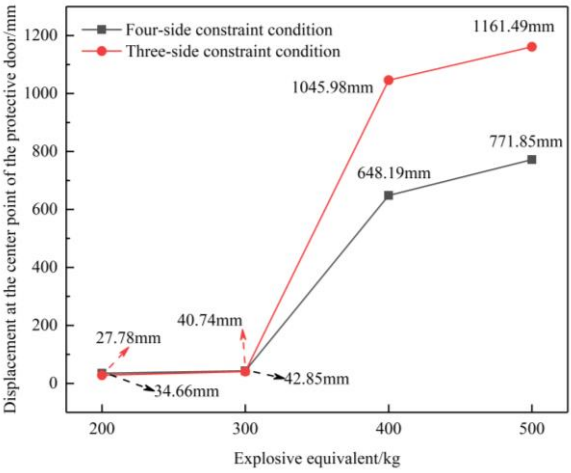

(b) Relationship between constraint conditions and maximum displacement

Fig. 6. Influence of different constraint conditions on the displacement at the center point

3.2 Influence of height and thickness of the flat web in the skeleton beam

To study the influence law of height and thickness of the flat web in the skeleton beam on the resistance of the protective door, we took the explosive equivalent as 500 kg and the initiation distance as 10 m, with other parameters kept unchanged. The original model was retained with the focus being on changing height (H) and thickness (t_w) of the flat web in the I-steel component, as illustrated in Table 4.

Table 4. Values of height and thickness of the flat web in the skeleton beam of the protective door

Working condition	Web height H (mm)				Web thickness t_w (mm)			
1	586				16	17	18	19
2	566	576	586	596	17			

As can be observed from Figures 7 (a) and (b), the change in the web height has little influence on the peak displacement at the center point of the protective door. With the increase of H, the displacement peaks were 786.28 mm, 776.47 mm, 771.85 mm, and 771.36 mm, respectively, with a decrease of only 1.9%. The reason is that the height of the support panel around the protective door changes with the change of web height, which also has a certain influence on the resistance of the protective door. As can be noted from Figures 8 (a) and (b), there was a clear trend of decreasing peak displacements of the protective door with the increase of web thickness. The recorded peak displacements were 822.12 mm, 771.85 mm, 717.04 mm, and 663.71 mm, respectively, reflecting a declining range of approximately 19.27%. These results indicate that increasing the web thickness has a notable influence on enhancing the anti-explosion performance of the protective door.

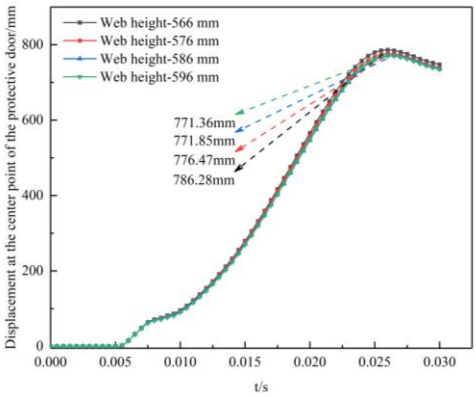

(a) Displacement time history curve of the center point of the protective door

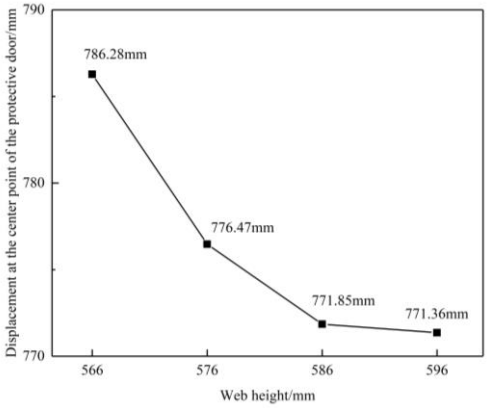

(b) Relation between web height and maximum displacement

Fig. 7. Influence of different web heights on the displacement at the center point

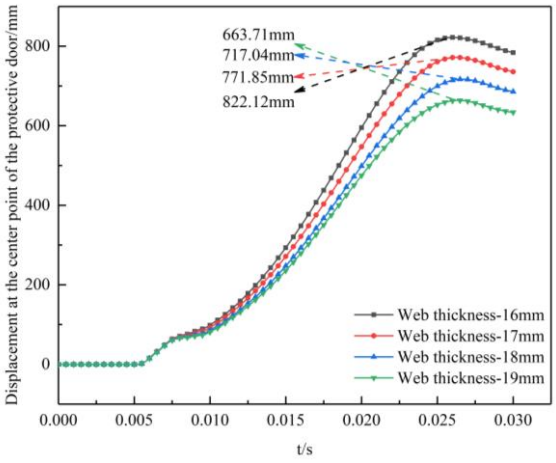

(a) Displacement time history curve of the center point of the protective door

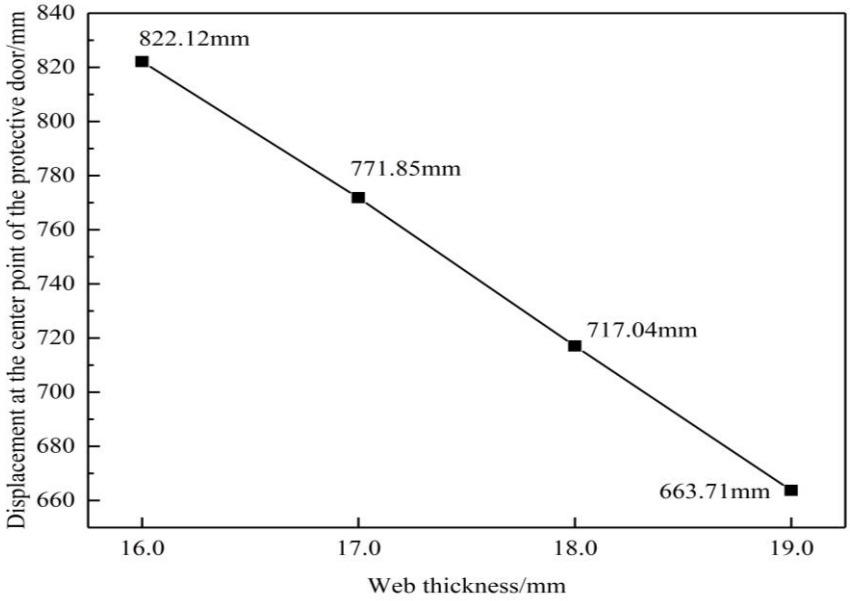

(b) Relation between web thickness and maximum displacement

Fig. 8. Influence of different web thicknesses on the displacement at the center point

3.3 Influence of width and thickness of flange plate of the skeleton beam

To investigate the influence of the width and thickness of the flange plate of the skeleton beam on the resistance of the protective door, we kept other parameters unchanged and only changed the width W and thickness t_f of the flange plate of I-steel based on the original model, as detailed in Table 5.

Table 5. Values of width and thickness of the flange plate of the skeleton beam on the protective door

Working condition	Flange plate's width W (mm)				Flange plate's thickness t_f (mm)			
3	180				21	22	23	24
4	160	170	180	190	22			

Based on the observations from Figures 9 (a) and (b) and Figures 10 (a) and (b), the change in the width and thickness of the flange plate has little effect on the resistance of the protective door. With the increase of flange width and thickness, the peak displacements were 776.85 mm, 770.29 mm, 771.85 mm, 812.27 mm and 783.23 mm, 771.85 mm, 769.44 mm, 774.99 mm, respectively. By and large, the flange plate only plays a role in fixing the upper and lower panels and preventing the flat web buckling of the skeleton beam, so it has little influence on the resistance of the protective door.

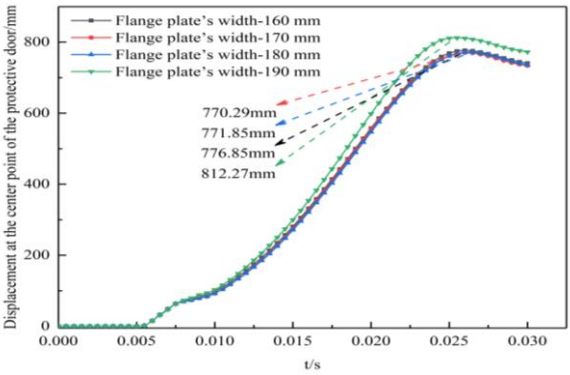

(a) Displacement time history curve of the center point of the protective door

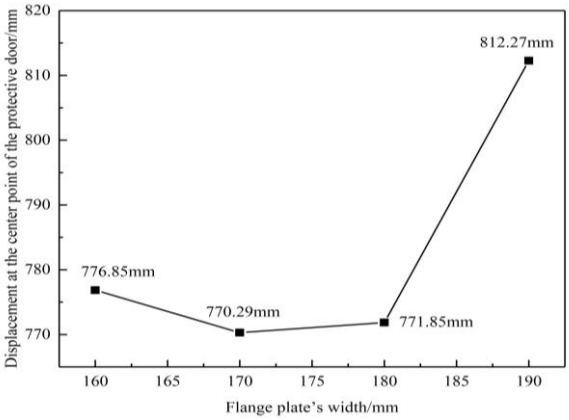

(b) The relationship between the width of the flange plate and the maximum displacement

Fig. 9. Influence of different widths of the flange plate on the displacement at the center point

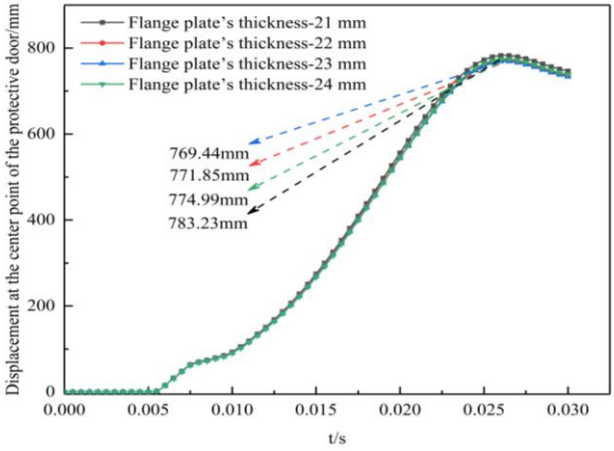

(a) Displacement time history curve of the center point of the protective door

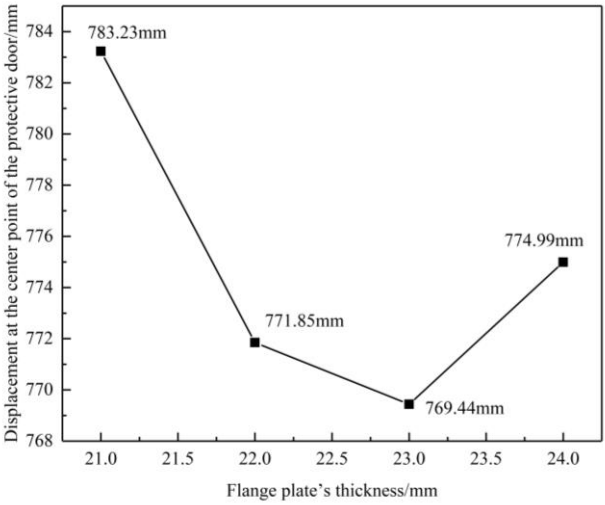

(b) The relationship between the thickness of the flange plate and the maximum displacement

Fig. 10. Influence of different thicknesses of the flange plate on the displacement at the center point

4 Conclusions

(1) The failure modes of steel beam-slab protective door under underwater explosion load can be classified into three categories: when the explosive equivalent ranges from 200 kg to 300 kg, the protective door presents local skeleton beam buckling failure; when the explosive equivalent exceeds 400 kg under the four-side simply supported constraint, the whole protective door exhibits bending failure, accompanied by compression-bending failure of the surrounding skeleton beams; when the explosive equivalent surpasses 400 kg under the three-side simply supported constraint, the protective door displays bending failure of skeleton beams on both sides, and serious warping failure occurs on both sides of the structure.

(2) The change of constraint conditions has a significant impact on the anti-explosion performance of the protective door. When the explosive equivalent is in excess of 400 kg, the failure under the three-side simply supported constraint is more severe compared to other constraint conditions. Consequently, it is advisable to avoid utilizing the three-side simply supported constraint in actual design scenarios.

(3) The height and thickness of the flat web in the skeleton beam have a substantial influence on the anti-explosion performance of the protective door. Increasing the thickness of the flat web in the skeleton beam can indeed improve the overall performance of the structure against the explosion. In contrast, the width and thickness of the flange plate have minimal influence on the resistance of the protective door.

References

1. Ren X, Wang Q, Chen Y, et al. (2022) Effects of bedrocks on the dynamic response of concrete gravity dams subjected to underwater explosions J. Engineering Failure Analysis, 139: 106410.
2. Chen L, Li S, Chen Y, et al. (2023) Study on damage effect of caisson wharves subjected to underwater explosion J. Ocean Engineering, 275: 113958.
3. Yang G D, Wang G H, Li Q, Lu C H, Lu W B, Zhou J R, Zhao J S. (2022) Study on dynamic response and failure mode of an underwater tunnel under explosion impact J. Vibration and shock, 41 (04): 150-158.
4. Guo D, Liu J B, Zhang X B. (2013) Dynamic response and resistance parameter analysis of steel protective door under explosion load J. Vibration and impact, 32 (03): 134-140 +156.
5. Li Z P, Guo D, Wang Q S, Hou X F. (2012) Analysis of dynamic response and door resistance parameters of steel protective door J. Protective Engineering, 34 (03): 25-32.
6. Hsieh M W, Hung J P, Chen D J. (2008) Investigation on the blast resistance of a stiffened door structure [J]. Journal of Marine Science and Technology, 16(2): 7.
7. Guo D, Liu J B, Yan Q S. (2011) Analysis of influencing factors of the rebound effect of the protective door under explosion load J. Engineering Mechanics, 28 (12): 206-212.
8. Jen C Y, Tai Y S. (2010) Deformation behavior of a stiffened panel subject to underwater shock loading using the non-linear finite element method J. Materials & Design, 31 (1): 325-335.
9. Jiang J, Olson M D. (1995) Rigid-plastic analysis of underwater blast loaded stiffened plates J. International journal of mechanical sciences, 37(8): 843-859.
10. Gupta N K, Kumar P, Hegde S. (2010) On deformation and tearing of stiffened and unstiffened square plates subjected to the underwater explosion—a numerical study J. International Journal of Mechanical Sciences, 52(5): 733-744.
11. Elsayed F, Qi H, Tong L L, et al. (2015) Optimal Configuration for Stiffened Plates under the Effect of Underwater Explosion. In Materials Science Forum. Trans Tech Publications Ltd. pp. 161-168.
12. Xiong G, Feng Y, Liao X D, et al. (2022) Lateral–torsional buckling behavior of welded Q690 steel I-beams with double lateral restraints along the length J. Thin-Walled Structures, 170: 108659.
13. Johnson G R, Cook W H. (1985) Fracture characteristics of three metals subjected to various strains, strain rates, temperatures and pressures J. Engineering fracture mechanics, 21(1): 31-48.
14. Yang X, Yang H, Zhang S. (2019) Rate-dependent constitutive models of S690 high-strength structural steel J. Construction and Building Materials, 198: 597-607.